Available online at www.sciencedirect.com
ScienceDirect
Journal of Molecular Catalysis A: Chemical 261 (2007) 172–179
JOURNAL OF MOLECULAR CATALYSIS A: CHEMICAL
www.elsevier.com/locate/molcata

Studies on heteropoly acid supported zirconia III: Oxidative bromination of phenol using phosphotungstic acid supported on zirconia

Sujata Mallik, K.M. Parida *, S.S. Dash

Colloids and Material Chemistry Cell, Regional Research Laboratory (CSIR), Bhubaneswar 751013, Orissa, India

Received 9 June 2006; received in revised form 25 July 2006; accepted 25 July 2006
Available online 11 September 2006

Abstract

A series of ecofriendly solid acid catalyst were synthesized by supporting phosphotungstic acid onto hydrous zirconia by an incipient wetness impregnation method in order to contribute towards clean technology. The support and resulting catalysts were characterized by various spectral and physicochemical techniques. Their catalytic activities were evaluated for oxybromination reaction of phenol by varying different reaction parameters. The electrophilic substitution of bromine generated in situ from KBr as a bromine source and hydrogen peroxide as an oxidant. The 15 wt.% of phosphotungstic acid supported on hydrous zirconia shows highest surface area, acid sites and gives about 93% conversion with 81% *para*-selectivity.

Keywords: Bromination; Potassium bromide; Hydrogen peroxide; *Para*-selectivity; Phosphotungstic acid and zirconia

1. Introduction

Selective bromination of aromatic compounds is investigated in view of the importance of the brominated compound in the synthesis of natural products and pharmaceutically important compounds [1]. Brominated arenes are versatile intermediates in the synthesis of a wide variety of biologically active compounds. Conventionally, a variety of methods for the bromination of aromatic have been reported in literature [2–12]. The traditional methods of aromatic bromination involve the use of non-selective hazardous acidic reagents such as mineral acids and metal halides, which can lead to separation difficulties and unacceptable levels of toxic and corrosive and waste materials [13–15].

The classical direct bromination of aromatic compounds suffers from being wasteful in the bromine employed; one half ends up as hydrogen bromide. In large scale operations this is an environmental as well as an economic problem. Oxybromination using HBr as a bromine source, H_2O_2 as an oxidant was thought to be possible solution to overcome these said difficulties. Since HBr is highly toxic, corrosive and harmful as that of molecular bromine to the environment, replacement of such reagents by non-toxic and more selective reagents is very desirable and represents a clean synthesis. So we have designed a heterogeneous catalytic system to generate electrophilic bromine in situ from easily available KBr as bromine source and H_2O_2 as an oxidant for the oxybromination as a possible alternative to solve the disadvantage described in the earlier method.

Heteropoly anions (HPA) have recently attracted attention as catalysts for various industrial processes such as oxidation, hydration, esterification and etheration [14,16]. These HPA are stronger acids and they have a significantly higher catalytic activity compared to homogeneous and acid catalysts such as sulphuric acid, silica-alumina or ion exchange resins. The use of HPA as catalysts is important in the development of clean technologies, since it avoids the drawbacks of environmental pollution and corrosion of the conventional technologies. Other advantage is the ability of recovering and reusing them in liquid phase reactions compared to the homogeneous catalysts and the possibility of their use in continuous processes.

The disadvantage of bulk HPA as catalysts is their relatively low stability and also of their low surface area (1–10 m^2/g). To minimize these disadvantages the HPA are usually supported on a carrier. Heteropoly acids supported on solids with high

* Corresponding author. Fax: +91674 2581637.
E-mail address: kmparida@yahoo.com (K.M. Parida).

1381-1169/$ – see front matter © 2006 Elsevier B.V. All rights reserved.
doi:10.1016/j.molcata.2006.07.073

surface area are also a useful method for improving catalytic performance.

The study of hydrous zirconia is of interest due to its special properties, which allow their use as catalyst or support. One of the main reasons that have drawn great attention to the use of hydrated zirconia as a precursor of a catalyst carrier is the fact that its surface hydroxyl groups are able to undergo a chemical reaction or strong interaction with incorporated components. Oxidative bromination of a range of aromatics with HBr in the presence of oxygen by Gorodetskaya et al. [17] over heteropoly acid and regioselective oxybromination of phenol with HBr gas by Neumann and Assael et al. [18] over $H_5PMo_{10}V_2O_{40}$ catalyst has been reported. The present work deals with the synthesis of phosphotungstic acid impregnated hydrous zirconia catalyst and its catalytic activity behavior towards the liquid phase oxybromination of phenol using easily available KBr as bromine source and H_2O_2 as an oxidant.

2. Experimental

2.1. Preparation of support, hydrous zirconia

Zirconium hydroxide gel was prepared from aqueous solution of zirconium oxychloride (Fine Chemical) by adding drop wise ammonium hydroxide solution (25% ammonia) (Merck) up to pH 9.5. The hydrogel was refluxed at room temperature for 24 h, then filtered and washed with deionized water and dried in an oven at 120 °C for 24 h (named Z herein after).

2.2. Preparation of phosphotungstic acid

Phosphotungstic acid was prepared by following steps. First $Na_2WO_4{\cdot}2H_2O$ (100 g) and $NaHPO_4{\cdot}12H_2O$ (50 g) were added to 160 ml decationized water and the mixture was refluxed at 80 °C with stirring. Then 24% HCl (150 ml) was added to the solution with stirring. Then the solution was evaporated to dryness at 50 °C.

2.3. Preparation of catalyst

The catalysts were prepared by wet impregnation method. A series of catalysts having different loading ranging from 3 to 20 wt.% were synthesized by impregnating 2 g of neat Z with an aqueous solution of phosphotungstic acid (PTA) (0.06–0.30 g/10–50 ml of conductivity water) under constant stirring followed by heating till complete evaporation of water takes place. Then it was dried in an oven at 120 °C for 24 h. The catalysts will be hereinafter referred to as *x*ZPTA (*x* = 3–20 wt.%). Catalysts with different PTA loading from 3 to 20 wt.% were then activated at various temperature for further study.

2.4. Physico-chemical characterization

The surface area measurement was carried out by BET method using Quantasorb instrument (Quantachrome, USA) by nitrogen adsorption–desorption measurements. The samples were degassed at 120 °C.

Surface acidity was determined spectrophotometrically on the basis of irreversible adsorption of organic bases such as pyridine (PY, $pK_b = 3.5$) and 2,6-dimethyl pyridine (DYPY, $pK_b = 8.7$) [6]. In this method, adsorption experiment was carried out in a 50 ml stoppered conical flask taking 10 ml of each freshly prepared adsorbate (Fluka, Switzerland) solution, along with 0.05 g of sample preheated at 120 °C with constant shaking. The concentration range for each adsorbate was varied from 0.005 to 0.01 M in cyclohexane (Merck). After 2 h the contents were filtered and absorbance of the filtrate was measured at preset wavelengths. For all cases, the sorption experiments were carried out in the adsorbate concentration range where Beer–Lambert's law was valid. The time required to reach equilibrium at room temperature was checked for all of the samples and was never more than 1 h. In other ward the time required for all the solute to adsorb on the active sites of the catalyst is optimum in 1 h. All the absorbance measurements were recorded in a spectrophotometer (Varian, Cary 1E) using 10 mm matched quartz cells.

The chemical interaction between the adsorbate and the catalyst may be described by the linear transferred Langmuir adsorption isotherm.

$$\frac{C}{X} = \frac{1}{b}X_m + \frac{C}{X_m}$$

where C is the concentration of organic substrate in solution in equilibrium with the adsorbate substrate, b a constant and X is the monolayer coverage, which corresponds to the theoretical amount of solute required to cover all the active sites for base adsorption.

The X-ray powdered diffraction pattern was recorded on a Philips PW 1710 diffractometer with automatic control. The patterns were run with a monochromatic Cu Kα radiation with a scan rate of $2^\circ\ min^{-1}$.

The FTIR spectra were taken using Jasco FTIR 5300 in KBr matrix in the range of 400–4000 cm^{-1}.

The UV–vis spectra of the samples were recorded in a Varian UV–vis-DRS spectrophotometer fitted with Carry 100 software. The spectra were recorded against the boric acid background.

Micrographs showing X-ray image mapping of different elements of washed manganese nodule leached residue were taken using a Japanese Model (JXA-8100) EPMA.

2.5. Catalytic reaction

Catalytic reaction was carried out in a 50 ml two necked round bottom flask, which charged with 0.2 g of catalyst (Phosphotungstic acid impregnated hydrous zirconia), phenol (2 mmol) in acetic acid (4 ml) and KBr (2.2 mmol). Thirty percent H_2O_2 (2.2 mmol) was then added drop wise to the reaction mixture. The content in the flask was stirred continuously at room temperature for 5 h (Scheme 1) [19].

After 5 h of the reaction, the catalyst was filtered and the solid was washed with ether. The combined filtrates were washed with saturated sodium bicarbonate solution and then shaken with

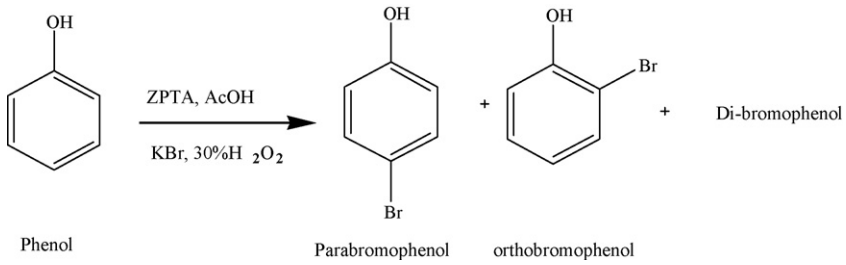

Scheme 1.

ether in a separating funnel. The organic extract was dried over anhydrous sodium sulfate. The products were analysed by GC (Shimadzu GC-17A) through capillary column at 210, 250 and 250 °C column, oven and detector temperature, respectively.

3. Results and discussion

3.1. Characterization

Table 1 shows the BET surface area of zirconia and different weight percentage of ZPTA samples in square meters per gram. The pure hydrous zirconia dried at 120 °C showed a surface area of 412 $m^2\ g^{-1}$.

With the increase in PTA content from 0 to 15 wt.%, the surface area increases from 412 to 523 m^2/g. However from 15 wt.% onwards, the surface area decreases gradually. This implies that the presence of PTA play a role in making the material porous. However, when the PTA content increases beyond 15 wt.%, pore blocking takes place due to the presence of an excess amount of phosphotungstic acid. With increase in activation temperature, the surface area decreases gradually. This might be due to the inter-particle agglomeration or due to collapse of very fine/narrow pore to form large pores.

Table 2 shows the surface acid sites of zirconia and different loading of PTA impregnated zirconia samples. Adsorption of pyridine (PY) measures the total acidity where as 2,6-dimethyl pyridine (DMPY) can be adsorbed on the BrØnsted acid sites. It is observed that by increasing the PTA loading up to 15 wt.% the acidity gradually increases (from 210 to 310 μmol/g), thereafter it decreases to 276 μmol/g for 20 wt.% ZPTA. The same trend also found for BrØnsted acid sites. The increase in surface acidity, with an increase in PTA loading may be due to the formation of monolayer coverage of PTA on zirconia. The decrease in the surface acidity at high PTA concentration is probably due to the formation of polylayer coverage of PTA on zirconia, which decreases the number of BrØnsted acid sites and consequently that of total acid sites. With increase in activation temperature, the strong acid sites as well as the BrØnsted acid sites decrease gradually.

From Fig. 1, it was observed that the XRD pattern of 15 wt.% ZPTA sample (dried at 120 °C) is similar to that of the support and shows no crystalline structure. This may be due to a high dispersion of solute on the support surface.

Table 1
Surface area of various PTA impregnated zirconia samples

Catalysts	Surface area ($m^2\ g^{-1}$)
Z	412.3
3 wt.% ZPTA—120 °C	459.0
6 wt.% ZPTA—120 °C	468.3
9 wt.% ZPTA—120 °C	475.9
12 wt.%ZPTA—120 °C	489.9
15 wt.%ZPTA—120 °C	523.6
20 wt.% ZPTA—120 °C	490.8
15 wt.% ZPTA—200 °C	456.9
15 wt.% ZPTA—300 °C	401.2
15 wt.% ZPTA—400 °C	354.4
15 wt.% ZPTA—500 °C	285.8

Table 2
Acid sites of various PTA impregnated zirconia samples

Catalysts	Acid sites (μmol/g)	
	PY	2,6 DMPY
Z	156.5	58.20
3 wt.% ZPTA—120 °C	210.2	97.5
6 wt.% ZPTA—120 °C	235.6	113.2
9 wt.% ZPTA—120 °C	251.3	165.6
12 wt.% ZPTA—120 °C	265.8	178.1
15 wt.% ZPTA—120 °C	310.1	211.9
20 wt.% ZPTA—120 °C	276.8	180.3
15 wt.% ZPTA—200 °C	300.2	199.3
15 wt.% ZPTA—300 °C	285.4	182.6
15 wt.% ZPTA—400 °C	280.6	171.1
15 wt.% ZPTA—500 °C	275.9	135.9

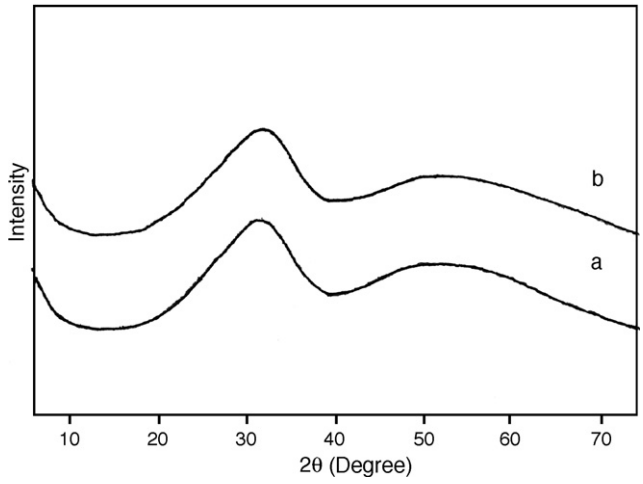

Fig. 1. XRD patterns of (a) Z, (b) 15 wt.% ZPTA (dried at 120 °C).

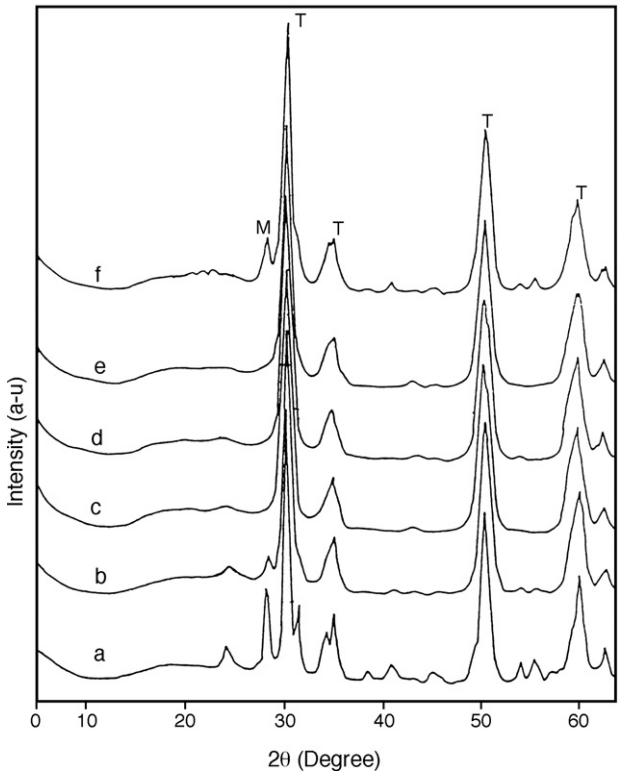

Fig. 2. XRD patterns of (a) Z, (b) 6 wt.% ZPTA, (c) 9 wt.% ZPTA, (d) 12 wt.% ZPTA, (e) 15 wt.% ZPTA and (f) 20 wt.% ZPTA (calcined at 500 °C).

Fig. 2 recorded after calcining the samples at 500 °C, it was observed that the pure zirconia contains tetragonal as well as monoclinic phases with the latter as the major constituents. For catalyst with low PTA loading, the XRD pattern can be described as the sum of monoclinic and tetragonal phases of zirconia. As (%) of loading of PTA increases, it shows increase in tetragonal phase while 15 wt.% ZPTA is showing completely tetragonal form of zirconia. This is due to monolayer coverage of PTA over zirconia. But on further increase in PTA loading, i.e. for 20 wt.% ZPTA, it shows monoclinic along with tetragonal phase.

Fig. 3 shows the background subtracted UV–vis-DRS spectra of (a) hydrous zirconia, (b) 15 wt.% ZPTA and (c) 15 wt.% ZPTA calcined at 500 °C samples. The hydrous zirconia (Fig. 3a) exhibits a strong absorption band at 230 nm, which may be attributed to the charge transfer from oxide species to zirconium cation ($O^- \rightarrow Zr^{4+}$). In contrast the spectra of both 15 wt.% ZPTA and 15 wt.% ZPTA calcined at 500 °C sample, show broad band at 260 nm, which match well with the reported figure [20], suggesting thereby the presence of undegraded $H_3PW_{12}O_{40}$ species. This indicates that the Keggin phase remains unaltered up to 500 °C.

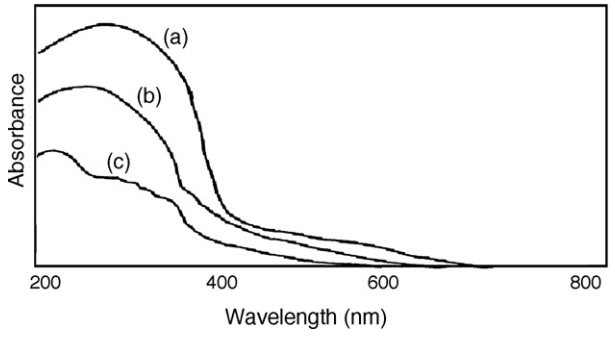

Fig. 3. DRS spectra of (a) Z, (b) 15 wt.% ZPTA, and (c) 15 wt.% ZPTA calcined at 500 °C.

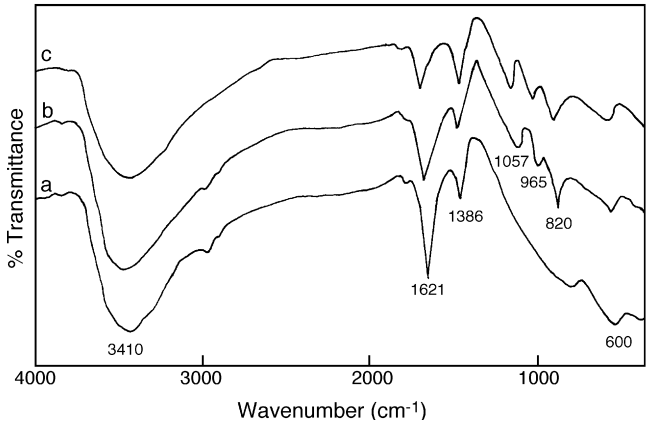

Fig. 4. FTIR spectra of (a) Z, (b) 15 wt.% ZPTA, and (c) 15 wt.% ZPTA calcined at 500 °C.

The FTIR spectra of hydrous zirconia and phosphotungstic acid impregnated on hydrous zirconia (15 wt.% ZPTA) are presented in Fig. 4a and b. The FTIR spectrum of Z (Fig. 4a) shows broadband in the region of 3410 cm^{-1} due to asymmetric stretching of OH group and two bands at 1621 and 1386 cm^{-1} are due to bending vibration of –(H–O–H)– and –(O–H–O)– bond. The band at 600 cm^{-1} is attributed to the presence of Zr–O–H bond. In addition to these bands, the FTIR spectra of 15 wt.% ZPTA (Fig. 4b) show bands at 820, 966 and 1072 cm^{-1}, which can be assigned to the symmetric stretching of (W–O–W), W=O, P–O, respectively [20].

The FTIR spectra of 15 wt.% ZPTA sample calcined at 500 °C is shown in Fig. 4c. There is slight shifting of bands, indicating that the Keggin phase remains unaltered upto 500 °C.

Fig. 5 shows the electron micrograph of haphazardly arranged zirconia crystallites. The electron micrograph of 15 wt.% ZPTA

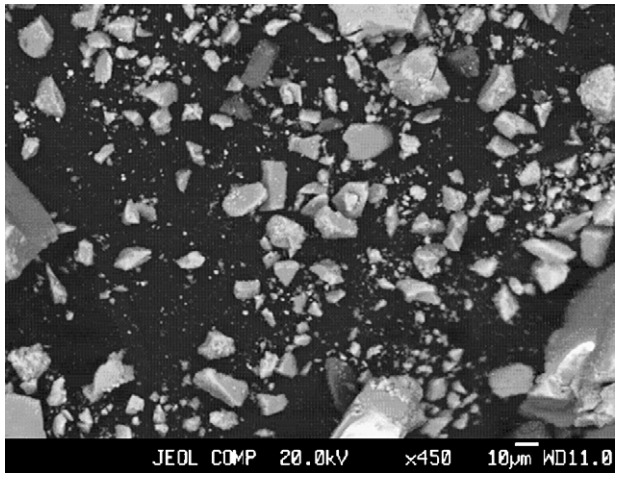

Fig. 5. Scanning electron micrograph of zirconia.

Fig. 6. Scanning electron micrograph of 15 wt.% ZPTA sample.

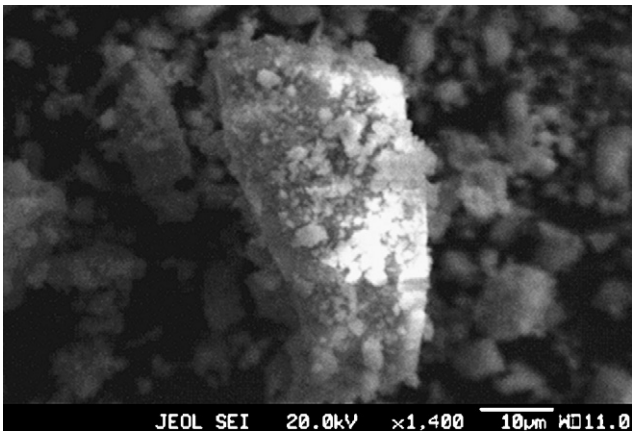

Fig. 7. Scanning electron micrograph of 15 wt.% ZPTA sample (single particle magnification at 1400×).

is shown in Fig. 6. The zirconia crystallites having tetragonal short columnar structure, is well observed in this figure. The enlarge view of ZPTA is shown in Fig. 7, where the fine particle of PTA are found to have adhered in the surface of zirconia.

Fig. 8 illustrates the X-ray image maps of W, P, Zr elements in a selected area (SL) showing their level of concentration through clustering of pixels. It can be seen from the maps that W is adsorbed in Zr grain more than that of phosphours. This is obvious since in original PTA, W content is 12 times more than phosphorus.

Fig. 9 illustrates the WDX spectra of 15 wt.% ZPTA sample showing the spectrum of W, P, Zr elements.

3.2. Bromination of phenol

Bromination is an acid catalyzed reaction. Various solvents including canbon tetrachloride, hexane, dichloromethane, methanol, acetonitrile and acetic acid was used for this reaction.

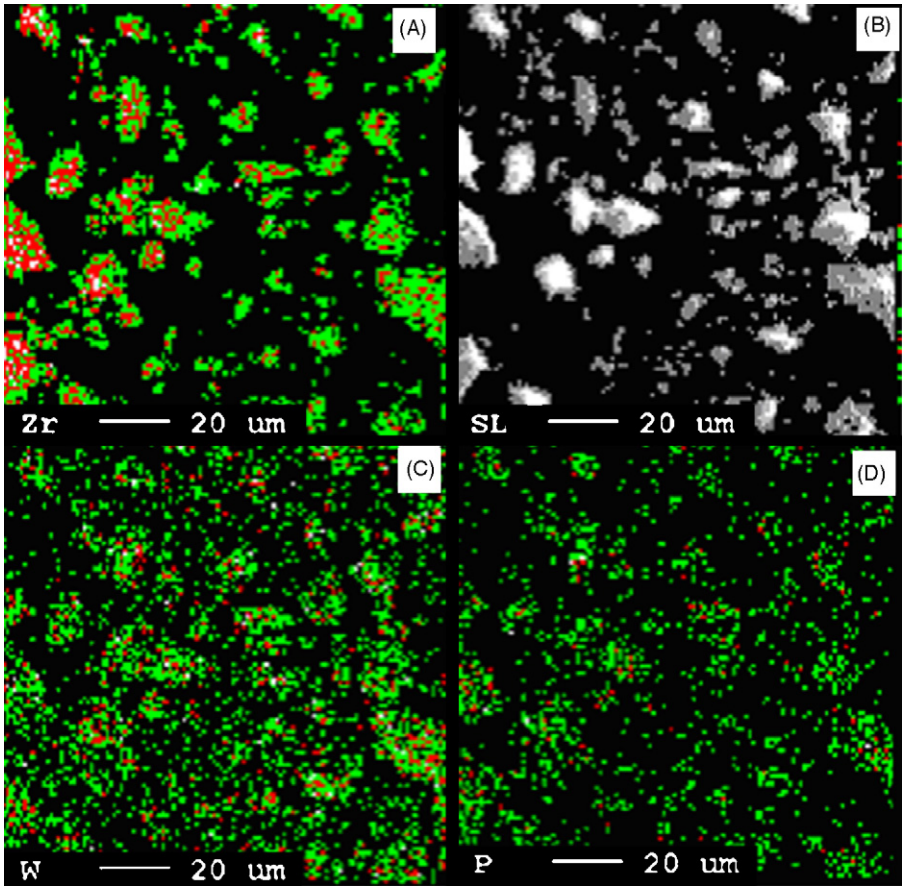

Fig. 8. Scanning electron micrograph of zirconia impregnated with 15 wt.% PTA sample. (A) X-ray image map of Zr, (B) secondary electron image of morphological view of 15 wt.% ZPTA, (C) X-ray image map of W and (D) X-ray image map of P.

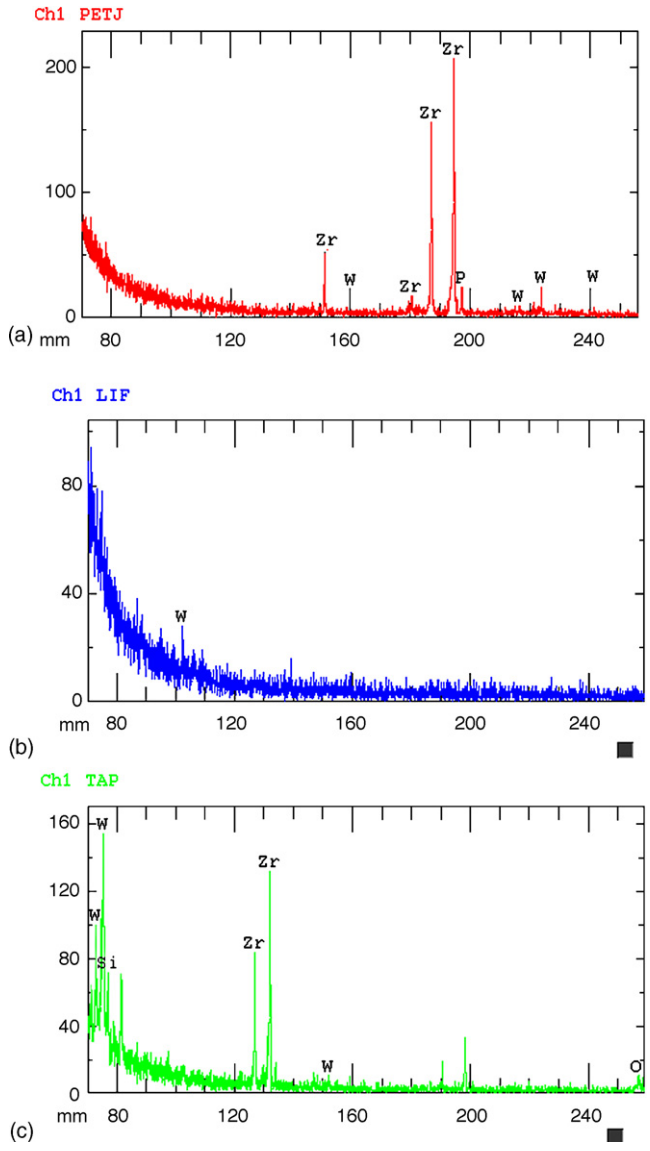

Fig. 9. WDX spectra of 15 wt.% ZPTA sample.

The best results were obtained when acetic acid was used as a solvent compared to others. In presence of H_2O_2, the acetic acid gives peracetic acid, which is stronger oxidant than H_2O_2 and efficiently oxidizes the Br^- to Br^+, which is not observed in case of other solvents.

It is assumed that the catalyst ZPTA reacts with hydrogen peroxide and forms peroxo species in presence of acetic acid [21]. The formed peroxo metal species then enhances the oxidation of Br^- (KBr) to Br^+ (HOBr), which reacts in presence of BrØnsted acidic centres of ZPTA with the organic substrate phenol to give, brominated compounds (Scheme 2).

We have investigated the use of various ZPTA as catalyst in different weight percentage, in the reaction of phenol with KBr and hydrogen peroxide at room temperature in acetic acid. The results show that all the catalysts were efficient for catalyzing the reaction. The selectivity of *para*-bromo, *ortho*-bromo and di-bromo phenol obtained is shown in Table 3.

Table 3
Conversion and selectivity of various catalysts towards oxybromination of phenol

Catalysts	*T* (h)	Conversion (%)	Selectivity (%)		
			Ortho-bromo	*Para*-bromo	Di-bromo
Z	5	48.84	34.48	65.52	–
3 wt.% ZPTA	5	65.00	41.05	58.94	–
6 wt.% ZPTA	5	72.30	38.85	61.15	–
9 wt.% ZPTA	5	77.34	34.80	65.20	–
12 wt.% ZPTA	5	82.19	29.81	70.17	–
15 wt.% ZPTA	5	93.34	18.54	81.06	0.30
20 wt.% ZPTA	5	83.75	19.66	79.21	1.12

Phenol (2 mmol), KBr (2.2 mmol), H_2O_2 (2.2 mmol), catalyst (200 mg) and acetic acid (4 ml), time 5 h.

From Table 3, it was found that the conversion was highest when 15 wt.% ZPTA was used as catalyst. The reaction over zirconia gives 48% of conversion having 34% *ortho*, 65% of *para*-selectivity in 5 h, whereas 15 wt.% ZPTA gave 93% conversion having 81% of *para*-bromo, 18% of *ortho*-bromo and 0.30% of di-bromo product.

From above data, it is assumed that phenol may interact with the Lewis acid sites of the catalyst as a result, the electron density at *ortho* positions of the aromatic ring decreased, which hinders the attack of incoming electrophile (Br^+) at two *ortho* position and preferred to attack on *para* position [22,23]. The variations of different reaction parameters were studied on 15 wt.% ZPTA catalyst.

Fig. 10 shows that with increase in calcinations temperature the percentage of conversion of phenol decreases but the selectivity towards *para*-bromo product increases. Narender et al. [19] reported that the formation of brominated product is mainly due to BrØnsted acid sites. With increase in the calcinations temperature, due to loss of BrØnsted acid sites (Table 2) the percentage of conversion decreases. The increase in selectivity of *para* product at higher calcinations temperature may be due to the presence of Lewis acid sites. Choudary et al. [24] reported that Lewis acid sites are mainly responsible for the *para*-bromo product.

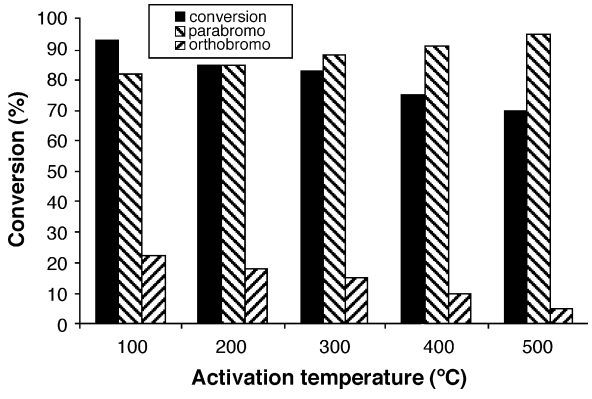

Fig. 10. Effect of activation temperature on conversion of phenol using 15 wt.% ZPTA as catalyst (0.2 g), phenol (2 mmol), KBr (2.2 mmol), H_2O_2 (2.2 mmol), and acetic acid (4 ml).

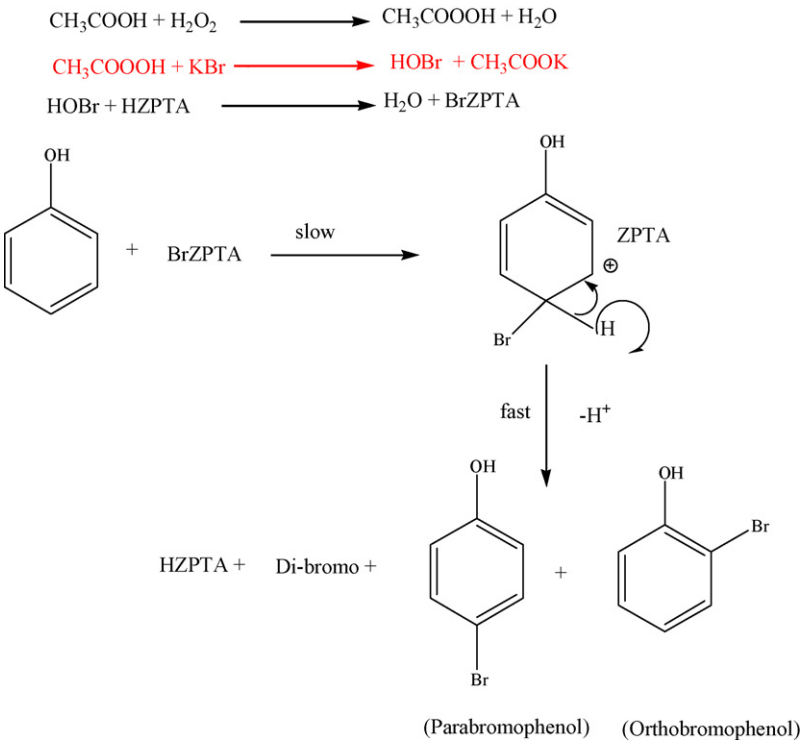

Scheme 2.

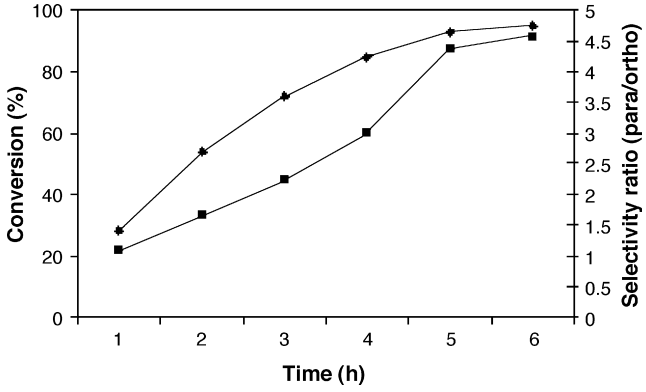

Fig. 11. Effect of time on conversion of phenol using 15 wt.% ZPTA as catalyst (0.2 g) Phenol (2 mmol), KBr (2.2 mmol), H_2O_2 (2.2 mmol), and acetic acid (4 ml).

Fig. 11 shows the effect of reaction time on percentage of conversion of phenol and selectivity ratio (*para*-bromo/*ortho*-bromo) using 15 wt.% ZPTA as catalyst (0.2 g) having similar reaction conditions. It was found that percentage of conversion of phenol increases from 28 to 93% with increase of reaction time from 1 to 5 h and then remains almost constant with further rise of reaction time up to 6 h. In case of selectivity (*para*-bromo/*ortho*-bromo), it increases from 1.09 to 4.56. In similar reaction conditions Narender et al. [19] reported the conversion in the range of 70–89% over modified zeolite as solid acid catalyst and the selectivity ratio (*para*-bromo/*ortho*-bromo) in the range of 1.29–2.32 (Table 4). Similarly the result reported by Singh et al. [8] and Parida et al. [25] have been compared with the present work in Table 4.

Fig. 12 shows the effect of concentration of catalyst on the percentage of conversion of phenol and selectivity of *para*-bromo/*ortho*-bromo under similar reaction conditions. When the catalyst amount increased from 0.05 to 0.4 g, the percentage of conversion of phenol and the selectivity ratio (*para*-bromo/*ortho*-bromo) increased from 45 to 96% and from 2.96 to 4.65, respectively. In case of *ortho*-bromo and di-bromo phenol no such trend was found.

3.3. Recyclability of the catalyst

The catalyst with 15 wt.% ZPTA was used for recycling experiments. In order to regenerate the catalyst after 5 h reaction

Table 4
Liquid phase bromination of phenol over 15 wt.% ZPTA and comparison of the result with other reported methods

Substrate	Catalyst used	Product	Conversion (%)	Reference
Phenol	ZPTA	*o*-BP, *p*-BP, di-BP	48–93% (*p*-BP/*o*-BP = 1.43–4.37)	This method
Phenol	Modified zeolite	*o*-BP, *p*-BP, di-BP	70–89% (*p*-BP/*o*-BP = 1.29–2.32)	[19]
Toluene	Zeolite	*o*-BP, *p*-BP, α-BT	49–67%	[8]
Phenol	Hydrotalcite	*o*-BP, *p*-BP, di-BP	55–82% (*p*-BP/*o*-BP = 1.29–1.7)	[25]

o-BP = *ortho*-bromophenol, p-BP = *para*-bromophenol, di-BP = di-bromophenol, α-BT = benzyl bromide.

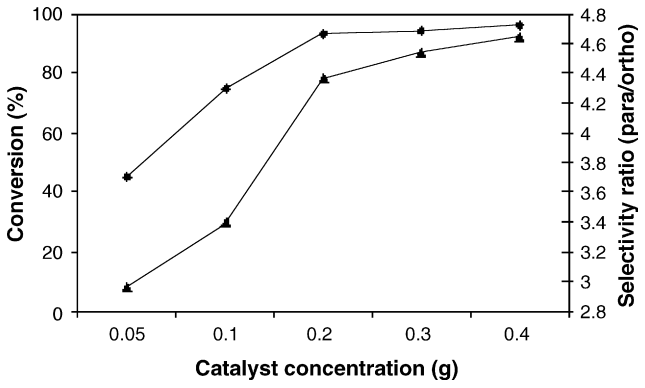

Fig. 12. Effect of concentration of catalyst amount on conversion of phenol using 15 wt.% ZPTA as catalyst, phenol (2 mmol), KBr (2.2 mmol), H_2O_2 (2.2 mmol), catalyst amount (200 mg) and acetic acid (4 ml).

time, it was separated by filtration, washed with conductivity water several times, dried and calcined at 120 °C and used in the oxybromination reaction with a fresh reaction mixture. In the regenerated sample after two cycles, the yield decreased by 5%.

4. Conclusions

Phosphotungstic acid supported on hydrous zirconia acts as an efficient and stable solid acid catalyst for oxybromination of phenol. FTIR spectra confirm that the phosphotungstic acid keeps its Keggin type structure when supported on zirconia up to 500 °C. EPMA studies show the dispersion of PTA anion into the surface of the support. In the oxybromination of phenol reaction, 15 wt.% of PTA impregnated on hydrous zirconia showed higher catalytic activity and having 81% *para* selectivity. The catalytic proficiency was found to be dependent on PTA concentration on the support. With increase in the catalyst concentration and reaction time (h), the *para*/*ortho*-selectivity ratio increased from 2.96 to 4.65 and from 1.09 to 4.56, respectively, was observed. In case of *ortho*-bromo and di-bromo phenol no such trend was found.

Acknowledgements

The authors are thankful to Prof. B.K. Mishra Director, Regional Research Laboratory (CSIR), Bhubaneswar, for his constant encouragement and permission to publish this paper. Financial assistant by CSIR to Mrs. Sujata Mallick is gratefully acknowledged.

References

[1] H. Konishi, K. Aritomi, T. Okano, J. Kiji, Bull. Chem. Soc. Jpn. 62 (1989) 591.
[2] Ulmann's Encyclopedia of Industrial Chemistry, sixth ed., Electronic Release, Wiley, Weinhein, 1998.
[3] P. Bovonsombat, E. Mcnelis, Synthesis (1993) 237.
[4] K. Smith, D. Bahzad, J. Chem. Soc. Chem. Commun. (1996) 467.
[5] V. Paul, A. Sudalai, T. Daniel, K.V. Srinivasan, Tetrahedron Lett. 35 (1994) 7055.
[6] J. Auerbach, S.A. Weissman, T.J. Blacklock, M.R. Angeless, K. Hoogstoen, Tetrahedron Lett. 34 (1993) 931.
[7] T. Oberhauser, J. Org. Chem. 62 (1997) 4504.
[8] A.P. Singh, S.P. Marajkar, S. Sharma, J. Mol. Catal. A 150 (1999) 241.
[9] Y. Goldberg, H. Alper, J. Mol. Catal. A 88 (1994) 377.
[10] N. Narender, P. Srinivasu, S.J. Kulkarni, K.V. Raghavan, Synth. Commum. 30 (2000) 2679.
[11] S.K. Srivastava, P.M.S. Chauhan, A.P. Bhaduri, J. Chem. Soc., Chem. Commun. (1996) 2679.
[12] J. Dakka, Y. Sasson, J. Chem. Soc., Chem. Commun. (1987) 1421.
[13] H. Lubbecke, P. Boldt, Tetrahedron 34 (1978) 1577.
[14] R. Neumann, I. Assael, J. Chem. Soc. Chem. Commun. (1988) 1285.
[15] Y. Izumi, K. Urabe, M. Onaka, Zeolite, Clay and Heteropoly Acid in Organic Reactions, Kodansha/VCH, Tokyo, 1992.
[16] I. Kozhevnikov, Catal. Rev. Sci. Eng. 37 (1995) 311.
[17] T.A. Gorodetskaya, I.V. Kozhovnikov, K.I. Matveev, USSR Patent 1,121,255 (1984).
[18] R. Neumann, I. Assael, J. Chem. Soc. Chem. Commun. (1988) 1285.
[19] N. Narender, K.V.V. Krishna Mohan, R. Vinod Reddy, P. Srinivasu, S.J. Kulkarni, K.V. Raghavan, J. Mol. Catal. A: Chem. 192 (2003) 73.
[20] T. Okuhura, N. Mizuno, M. Misono, Adv. Catal. 41 (1996) 113.
[21] J. Muzart, Chem. Rev. 92 (1992) 113.
[22] A.F. Holleman, Chem. Rev. (1924) 178.
[23] R. Breslow, P. Campbell, J. Chem. Soc. 91 (1969) 3035.
[24] B.M. Choudary, t. someshwar, Ch. Venkat Reddy, M. Lakshmi Kantam, K. Jeeva Ratnam, L.V. Sivaji, Appl. Catal. A 251 (2003) 397.
[25] K.M. Parida, S. Parija, J. Das, P.S. Mukherjee, Catal. Commun. 7 (2006) 915.